HHS Public Access

Author manuscript

Clin Sci (Lond). Author manuscript; available in PMC 2022 July 05.

Published in final edited form as:

Clin Sci (Lond). 2022 June 17; 136(11): 879–894. doi:10.1042/CS20220117.

Hypertension induces gonadal macrophage imbalance, inflammation, lymphangiogenesis, and dysfunction

Shobana Navaneethabalakrishnan,

Brooke K. Wilcox,

Bethany L. Goodlett,

Malea M. Murphy,

Brett M. Mitchell

Department of Medical Physiology, Texas A&M College of Medicine, Bryan, Texas 77807, U.S.A.

Abstract

Hypertension (HTN) is associated with gonadal dysfunction and impaired reproductive health in both men and women. An imbalance in the systemic and renal proinflammatory (M1)/anti-inflammatory (M2) macrophage ratio, increased inflammation, and inflammation-associated lymphangiogenesis have been observed in animals with HTN. However, the impact of HTN on gonadal macrophages, inflammation, and lymphatics remains obscure. We hypothesized that salt-sensitive HTN (SSHTN) and HTN alters gonadal macrophage polarization, which is associated with inflammation, inflammation-associated lymphangiogenesis, and reproductive dysfunction. Flow cytometry analyses revealed a significant increase in M1 macrophages in the testes of SSHTN and nitro-L-arginine methyl ester hydrochloride (L-NAME)-induced HTN (LHTN) mice, with a concurrent decrease in M2 macrophages in SSHTN mice yet an increase in M2 macrophages in LHTN mice. Ovaries from SSHTN mice exhibited an increase in M1 and a decrease in M2 macrophages, while ovaries from LHTN mice had a significant increase in M2 and a decrease in M1 macrophages. Gene expression patterns of proinflammatory cytokines revealed gonadal inflammation in all hypertensive mice. Increased lymphatic vessel density in the gonads of both male and female hypertensive mice was confirmed by immunofluorescence staining for lymphatic vessel endothelial hyaluronan receptor 1 (LYVE-1). HTN adversely affected the expression pattern of steroidogenic enzymes, hormone receptors, and secretory proteins in both the testes and ovaries. In line with these results, male hypertensive mice also presented with decreased sperm concentration, and increased percentage of sperm with abnormal morphology, damaged acrosome, and nonfunctional mitochondrial activity. These data demonstrate that HTN alters

Correspondence: Brett M. Mitchell (brettmitchell@tamu.edu).

Competing Interests

The authors declare that there are no competing interests associated with the manuscript.

CRediT Author Contribution

Shobana Navaneethabalakrishnan: Conceptualization, Data curation, Software, Formal analysis, Funding acquisition, Investigation, Visualization, Methodology, Writing–original draft, Writing–review & editing. **Brooke K. Wilcox:** Data curation, Software, Formal analysis, Investigation, Methodology, Writing–review & editing. **Bethany L. Goodlett:** Data curation, Software, Formal analysis, Validation, Investigation, Visualization, Methodology, Writing–review & editing. **Malea M. Murphy:** Data curation, Investigation, Visualization, Methodology. **Brett M. Mitchell:** Conceptualization, Resources, Data curation, Formal analysis, Supervision, Funding acquisition, Investigation, Project administration, Writing–review & editing.

gonadal macrophage polarization, which is associated with gonadal inflammation, inflammation-associated lymphangiogenesis, and dysfunction.

Introduction

Hypertension (HTN), affecting nearly 50% of the population, is the primary risk factor contributing to cardiovascular disease, accounting for over half a million deaths in the United States each year [1,2]. Individuals with HTN are not only susceptible to serious health issues like stroke, kidney disease, and heart failure but also experience impaired sexual health [3,4]. Erectile dysfunction, reduction in semen volume, serum testosterone, sperm count and motility, and an increase in abnormal sperm morphology are conditions described in hypertensive men [4–7]. Similarly, hypertensive females exhibit decreased vaginal lubrication, reduced orgasm, and several complications during pregnancy leading to fetal and maternal morbidity and mortality [8–10]. These impairments in reproductive health have been ascribed primarily to attenuated levels of hormones and altered vasculature of reproductive organs [11–15]. However, the detailed molecular mechanisms underlying the reproductive dysfunction associated with HTN remain obscure.

Studies in humans and animals have established a strong link between systemic inflammation and HTN [16–20]. Macrophages are one of the most abundant immune cells that are implicated in the chronic, low-grade inflammation associated with HTN [21]. It is shown that genetic deletion of monocytes/macrophages prevents HTN [17,22,23]. Our lab and others have demonstrated previously increased macrophages, inflammation, and inflammation-associated lymphangiogenesis in the kidneys of mice with HTN and salt-sensitive HTN (SSHTN) [24–29]. The heterogeneity and plasticity of macrophages permit them to perform various tissue-specific functions by switching between proinflammatory (M1) and anti-inflammatory (M2) phenotypes [30]. In HTN and SSHTN, circulating monocytes and resident macrophages have been reported to possess a tendency to polarize toward M1 phenotype in kidneys and other organs [31–36]. Nevertheless, it is unknown whether HTN alters gonadal M1/M2 macrophage ratios and if this is associated with inflammation, inflammation-associated lymphangiogenesis, and gonadal dysfunction.

Based on the limited studies available, we hypothesized that SSHTN and HTN increases M1 macrophages in the gonads, which is associated with inflammation, inflammation-associated lymphangiogenesis, and gonadal dysfunction. To test the above hypothesis, the study employed two models of HTN that simulate humans with SSHTN and hypertensive patients with elevated levels of the endogenous nitric oxide synthase inhibitor asymmetric dimethylarginine. Here, we report the effect of SSHTN and HTN on male and female gonadal macrophage polarization, inflammation, lymphatics, and function.

Methods

Animal models

All the experimental protocols performed at College of Medicine, Texas A&M University were approved by the Texas A&M University (IACUC: 2022-0083) in accordance with the

NIH Guide for the Care and Use and Care of Laboratory Animals. Wild-type C57BL/6J mice were purchased from Jackson Laboratories (Bar Harbor, ME). Male and female mice 10–14 weeks of age were made hypertensive by either providing nitro-L-arginine methyl ester hydrochloride (L-NAME) (0.5 mg/ml; Sigma, St. Louis, MO), a nitric oxide synthase inhibitor in the drinking water for 2 weeks, followed by a 2-week washout period and a subsequent 3-week 4% high-salt diet (Teklad Envigo, Huntingdon, U.K.) (SSHTN) or by providing L-NAME in their drinking water for 3 weeks (LHTN) [26,28]. Control mice received a normal diet and tap water *ad libitum*. Mice were euthanized after the completion of treatment period by exsanguination under 5% inhalational isoflurane anesthesia with death confirmed by cervical dislocation before tissue collection.

Blood pressure measurements

Systolic blood pressure (SBP) was measured weekly using the IITC Life Science (IITC Inc, Woodland Hills, CA, U.S.A.) noninvasive tail-cuff blood pressure acquisition system. The entire procedure was performed in a designated quiet area, and mice were acclimatized for 30 min. The restrainers and warming chambers were preheated to 34°C. Mice were gently placed into a restrainer of appropriate size and acclimatized for 5 min in the warming chamber prior to SBP recordings. SBP values were determined from the blood pressure traces by blinded investigators.

Flow cytometry

Testes/ovaries were collected, minced with scissors, and digested in buffer with Collagenase II (1 mg/ml) (Worthington Biochemicals, Lakewood, NJ, U.S.A.), DNAase I (0.15 mg/ml) (Sigma) and Dispase II (1 mg/ml) (Sigma, St. Louis, MO, U.S.A.) at 37°C for 30 min in gentle MACS™ Octo dissociator with heaters (Miltenyi Biotec, San Diego, CA, U.S.A.). Samples were filtered and rinsed with Dulbecco's phosphate-buffered saline (DPBS; Thermo Fisher Scientific, 14190250) through sterile 100 and 40 μm strainers. The cellular components were isolated by centrifugation, and red blood cells were lysed in ACK lysis buffer (Thermo Fisher Scientific, Waltham, MA, U.S.A.). Cells were resuspended in RPMI 1640 (Roswell Park Memorial Institute) media (containing 10% fetal bovine serum v/v, 100 IU/ml penicillin/streptomycin) to stop lysis, centrifuged and rinsed twice with DPBS. For immunophenotyping of macrophages in testes/ovaries, single-cell suspensions were stained for 30 min with Ghost red 710 viability dye (Tonbo Bioscience, San Diego, CA). Following washing with DPBS, cells were subsequently Fc blocked by using an antimouse CD16/CD32 antibody (BD Pharmingen, San Jose, CA) for 10 min on ice. Next, cells were stained using fluorescent-conjugated antibodies against CD45, CD11b, F4/80, CD11c, and CD206 (1:50 and 1:100 dilutions of antibodies were used for testes and ovaries, respectively). All antibodies were purchased from either Biolegend (San Diego, CA) or BD Biosciences (San Jose, CA). See Supplementary Table S1 for descriptive panel. Populations of up to 1×10^6 total cells were analyzed. Acquisition was performed on a BD LSR Fortessa X-20 flow cytometer using FACS DIVA software (BD Biosciences, San Jose, CA). Analysis was performed using Flow Jo v 10.7.1 (FlowJo, LLC, Ashland, OR). Macrophage populations were quantified within the $CD45^+CD11b^+F4/80^+$ gate and identified as M1 ($CD45^+CD11b^+F4/80^+CD11c^+CD206^{low}$) or M2 ($CD45^+CD11b^+F4/80^+CD11c^-CD206^+$) cells in testes as described previously [37]; M1 ($CD45^+CD11b^+F4/80^+CD11c^+CD206^-$)

or M2 ($CD45^+CD11b^+F4/80^+CD11c^-CD206^+$) cells in ovaries as described previously [38]. Results are expressed as a percentage of $CD11b^+F4/80^+$ cells per animal. Unstained specimen and compensation control were used for all relevant samples to justify gating strategy. Fluorescence minus one (FMO) control was used wherever needed.

Real-time quantitative PCR

Testes/ovaries were homogenized, and total RNA was isolated using the Quick-RNA mini prep kit (Zymo Research, Irvine, California, U.S.A.) following the manufacturer's instructions. cDNA synthesis was performed using 0.5 μg total RNA by following the manufacturer's instructions provided by the Qiagen RT^2 First Strand kit (Germantown, Maryland, U.S.A.). Ten microliter of qRT-PCR reactions was carried out using SYBR Green ROX qPCR Mastermix (Qiagen), nuclease-free water (Invitrogen, Carlsbad, California, U.S.A.), and primers (10 μM) (Sigma-Aldrich, St. Louis, Missouri, U.S.A.) along with cDNA from testes/Ovaries. Reactions were run in duplicate using the QuantStudio6 Flex Real-Time PCR system (Applied Biosystems, Foster City, California, U.S.A.). All the data were normalized to the expression levels of Ubiquitin (*Ubc*) and fold-changes were calculated using the $2^{-\Delta\Delta CT}$ method. The primers used in the current study are shown in Supplementary Table S2.

Immunofluorescence

Testes/ovaries were dissected and fixed in 4% PFA (Sigma) for 24 h. Tissues were then rinsed with phosphate-buffered saline (PBS) and stored in 70% ethanol until they were embedded in paraffin. Five-micrometer tissue sections were deparaffinized, rehydrated, and permeabilized with 0.1% Triton solution. The tissue sections were then blocked with 10% AquaBlock (EastCoastBio, North Berwick, Maine, U.S.A.) for 1 h at room temperature and were incubated with antibodies against lymphatic endothelial cell marker, lymphatic vessel endothelial hyaluronan receptor 1 (LYVE-1) (Goat polyclonal, R&D Systems, Minneapolis, MN, U.S.A.) and endothelial cell marker, platelet endothelial cell adhesion molecule 1 (PECAM-1), also known as CD31 (Rabbit polyclonal, Abcam, Cambridge, U.K.) at 4°C overnight. Alexa Fluor 488 or 594 secondary antibodies (Life Technologies, Carlsbad, California, U.S.A.) were used for visualization by incubating the sections at room temperature for 1 h. Sections incubated with only secondary antibody served as negative controls. Labeled slides were mounted with Prolong Gold antifade reagent with DAPI (Thermo Fisher Scientific, Waltham, Massachusetts, U.S.A.) and imaged using an Olympus BX51 fluorescence microscope with Olympus Q5 camera. Images were captured at 4× and 10× magnification using the Olympus CellSens software (Olympus, Shinjuku, Tokyo, Japan). For quantification of LYVE-1+ lymphatic vessels, four images from predetermined areas at outer tunica albuginea area in testes sections were captured at 10× magnification, by two independent, blinded investigators. In ovaries, images were captured at 4× magnification. The area values measuring total number of LYVE-1+ pixels were determined using ImageJ software (NIH, Rockville, MD) after setting the threshold for positive endothelium.

Tissue clearing and 3-D imaging

Tissue clearing was carried out using the previously described method [39]. Briefly, mice were anesthetized under 5% isoflurane and perfused with 20 ml of PBS and 30 ml of 4% PFA in PBS through the left ventricle of the heart. Testes/ovaries were dissected out and fixed in 4% PFA at 4°C for 24 h, then washed with PBS for 2 h, thrice at room temperature. Then, the fixed organs were immersed in 50% (v/v) CUBIC-L (1:1 mixture of water and CUBIC-L) for 6 h and then switched to 100% CUBIC-L with shaking at 37°C for 5 days, refreshed daily. Testes/ovaries were washed with PBS for 2 h, thrice after the delipidation process. The samples were then stained with primary antibody against the lymphatic endothelial cell marker, LYVE-1 (Goat polyclonal, R&D Systems, Minneapolis, MN, U.S.A.), in the staining buffer containing 0.5% Triton X-100, 0.5% casein (Thermo Fisher Scientific, Waltham, MA, U.S.A.) and 0.05% sodium azide (Sigma) for 7 days at 37°C with shaking. Testes/ovaries were then washed with 0.5% triton X-100 in PBS (PBST) for 1 day, and then stained with Alexa Flour 488 secondary antibody (Life Technologies, Carlsbad, California, U.S.A.) in the staining buffer consisting of 0.5% Triton X-100, 0.1% casein, and 0.05% sodium azide for 7 days at 37°C with gentle shaking. After staining the samples were washed with PBST for 1 day and fixed in 1% formaldehyde solution for 3 h, followed by PBS wash for 2 h, thrice. Finally, the refractive index was matched by immersing the samples in 50% (v/v) CUBIC-R+ (1:1 mixture of water and CUBIC-R+) for 1 day and in 100% CUBIC-R+ with gentle shaking for 2 days. The confocal images were acquired using Olympus Fluoview 3000 laser scanning confocal microscope (Olympus, Tokyo, Japan) at 10× magnifications with excitation wavelengths of 488 nm for imaging lymphatic vessels. All raw image data were collected in a 16-bit TIFF format. 3D-rendered images were visualized, captured, and analyzed with Imaris software (Bitplane, Switzerland).

Sperm concentration, motility, and morphology

Caudal epididymides from each animal were snipped and placed in 2 ml of preheated (37°C) Biggers-Whitten-Whittingham (BWW) media. The caudal portions were punctured three- to four-times with a 27-gauge needle and incubated for 10 min to allow the sperm to swim out. For determining sperm concentration, 10 µl of the diluted spermatozoa (1:20) was added to each side of a Neubauer chamber and counted under light microscope (400×) and the results were expressed as million sperm/ml. Sperm motility was assessed immediately by placing 10 µl of diluted sperm suspension on prewarmed microscope slide and covered with a cover slip. Two hundred spermatozoa per animal were evaluated under light microscope (400× magnification) for motility and expressed as the % motile cells. Sperms that moved forward were considered and those with *in situ* movement were excluded. For the assessment of sperm morphology smears were stained with hematoxylin-eosin. A total of 200 spermatozoa per mouse were evaluated under light microscope, using 400× magnification and sperm with abnormalities, such as lack of a hook, having amorphous, banana-shaped heads, folded heads, being twin tailed, or having twin heads, were recorded.

Sperm acrosome integrity and mitochondrial activity

Sperm acrosome integrity was assessed using a fluorescent-labeled peanut agglutinin (FITC-PNA) (Sigma-Aldrich) as described previously [15]. Briefly, smears of sperm suspension were fixed in methanol for 15 min, air-dried, and stained with FITC-PNA (60 μg/ml in PBS) in the dark for 30 min. Slides were then washed with Milli-Q water to remove excessive staining. Two hundred spermatozoa were evaluated under Olympus Fluoview 3000 confocal microscope at 600× magnification and classified as intact or damaged acrosome based on the staining since FITC-PNA binds exclusively to the outer acrosomal membrane.

Sperm mitochondrial activity was assessed using a fluorescent dye Rhodamine 123 that is rapidly taken up by functional mitochondria. In brief, 5 μl of Rhodamine 123 (Sigma, U.S.A.) solution (1 mg/ml in DMSO) was added to 1 ml of diluted sperm suspension and incubated for 10 min at 25°C in the dark. Following incubation, the supernatant was removed by centrifugation (300× *g*, 10 min) and the sperm pellets were resuspended in 1 ml PBS. A drop of 10 μl of the suspension was placed on microscopic slides, covered with coverslips, and examined at 400× magnification under Olympus BX51 fluorescence microscope with Olympus Q5 camera. A total of 200 spermatozoa were examined per animal and expressed as percentage of mitochondrial activity.

Statistical analysis

Statistical analysis was performed using GraphPad Prism, version 8.4.3. Data are presented as bar graphs/dot plots representing the mean ± SEM. Two-tailed Student's *t* test was used to assess data between the groups and the significance level was set at $P<0.05$. Statistical test and number of animals in each group are indicated in each figure panel or legend.

Results

SSHTN increases M1 macrophages and is associated with inflammation, and increased lymphatics in both testes and ovaries

To evaluate the direct impact of SSHTN on the gonads, mice were administered L-NAME in their drinking water for 2 weeks, followed by a washout period of 2 weeks, and then provided a 4% high-salt diet for 3 weeks as described previously [26]. As expected, both male (Figure 1A) and female (Figure 1B) mice developed SSHTN. There were no differences in the body weights of male and female mice and relative weight of ovaries, but there was a significant increase in the relative weight of testes in SSHTN mice (Supplementary Table S3). To investigate gonadal macrophage changes in SSHTN, we immunophenotyped gonadal cell populations by flow cytometry. The data revealed a significant increase in M1 macrophages and a significant decrease in M2 macrophages in both the testes (Figure 1C) and ovaries (Figure 1D) of mice with SSHTN when compared with control mice. Since SSHTN is well associated with inflammation, we then examined whether SSHTN promotes inflammation in the gonads, for which we measured the gene expression of proinflammatory mediators. We found a significant increase in the mRNA expression of the proinflammatory mediators *Il1b, Il6, Il17, Tnfa, Ifng*, and *Nos2* in the testes of mice with SSHTN (Figure 1E). Ovaries from SSHTN mice demonstrated significantly increased expression of *Il6, Il17*, and *Nos2* (Figure 1F).

We have previously reported that HTN and SSHTN is well associated with immune cell infiltration, inflammation, and inflammation-associated lymphangiogenesis in kidneys [28,29]. Nonetheless, it is largely unknown whether the same happens in the gonads of hypertensive subjects. We therefore examined gonadal lymphatic vessel density by performing immunofluorescence on testis and ovary sections by staining for the lymphatic vessel marker LYVE-1. Quantification of LYVE-1+ pixels per field confirmed a significant increase in lymphatic density in both testes (Figure 2A) and ovaries (Figure 2B) of SSHTN mice when compared with control mice. In support of these results, we also found significantly increased gene expression of the lymphatic markers *Lyve1, Prox1* (a lymphatic endothelial cell transcription factor), *Pdpn* (podoplanin), *Vegfc* (vascular endothelial growth factor C), *Vegfd* (vascular endothelial growth factor D), *Vegfr2* and *Vegfr3* (the receptors for the lymphangiogenic growth factors VEGF-C and VEGF-D), and adhesion molecules such as *Icam* and *Vcam* in the testes of SSHTN mice (Figure 2C). Testes from SSHTN mice also had an increase in the lymphatic-expressed immune cell-trafficking chemokine *Ccl21* and its receptor *Ccr7* (Figure 2C). Ovaries from SSHTN mice also exhibited increased expression of the lymphatic markers *Lyve1, Prox1, Pdpn, Vegfc, Vegfr2, Vegfr3*, and the lymphatic-expressed immune cell-trafficking chemokine *Ccl19* (Figure 2D). 3-D model and reconstruction of confocal images of LYVE-1+ lymphatic vessels in both testes and ovaries from the control and SSHTN mice can be observed in Figure 2E–H and Supplementary Videos S1–S4, respectively. The quantification of LYVE-1+ lymphatic vessels in CUBIC cleared gonads are given in Supplementary Table S5. Together, these results demonstrate that SSHTN in both males and females induces a significantly increased M1 and decreased M2 macrophages in the gonads, and this is associated with inflammation and inflammation-associated lymphangiogenesis.

SSHTN impairs gonadal function

The two critical functions of testes are steroidogenesis [production of testosterone (T)] and spermatogenesis [formation of haploid germ cells (GCs)] [40,41]. These functions are tightly regulated by gonadotropins, luteinizing hormone (LH) that acts on T-producing Leydig cells (LCs) present in the interstitial compartment, and follicle-stimulating hormone (FSH) that acts on Sertoli cells (SCs) in the seminiferous tubule [40,41]. The process of steroidogenesis involves a cascade of complex enzymatic reactions that are catalyzed by two classes of enzymes, cytochrome P450 (CYP) and hydroxysteroid dehydrogenases (HSD), where cholesterol is converted into a biologically active steroid hormone [42]. To uncover the basis of gonadal dysfunction observed in HTN, we analyzed the expression of steroidogenesis pathway genes. The mRNA expression of the steroidogenic acute regulatory protein *Star,* a rate-limiting protein that controls cholesterol transport, was decreased significantly in the testes of SSHTN mice (Figure 3A). There was also a significant decrease in the expression of *Hsd3b1* and *Hsd17b1* in the testes of SSHTN mice (Figure 3A). The expression of *Cyp17a1* was decreased in the testes of mice with SSHTN, whereas *Cyp11a1* remained unchanged (Figure 3A). We next investigated the effect of SSHTN on hormone signaling and analyzed the expression pattern of hormone receptors that regulate steroidogenesis and spermatogenesis. We found that SSHTN caused a significant decrease in the expression of androgen receptor (*Ar*), estrogen receptor subtype a *(Era),* and *Lhr,* whereas *Fshr* and estrogen receptor b (*Erb*) were not altered in the testes (Figure 3A).

The process of spermatogenesis is under the regulation of T and FSH that acts on SCs, which in turn supplies nutrients and growth factors and provides structural support for the developing GCs [40,43]. To investigate the effect of SSHTN on the secretory activity of SCs, we studied the gene expression of a few secretory proteins. Notably, there was a significant increase in the expression of *Inhba* (Activin A) and *Scgb1b24* (androgen-binding protein, ABP) along with a significant decrease in the expression of *Inhbb* (Inhibin B) and *Trf* (Transferrin) in the testes of SSHTN mice (Figure 3B). These results highlight the modulating effect of SSHTN on the secretory activity of the testes.

Apart from supplying nutrients and growth factors, SCs also provide a structural barrier called the blood–testis barrier (BTB) that regulates the flow of nutrients and sequesters the developing GCs from the host immune system. The BTB comprises mainly tight junctions (TJs), gap junctions, and adherens junctions [43]. TJs comprises TJ proteins (TJPs) that play a crucial role in maintaining an intact BTB and are under the control of hormones, mainly T and FSH [44,45]. To explore whether SSHTN affects BTB, we examined the expression of key TJPs in the testes. Mice with SSHTN had significantly decreased testes gene expression of the TJPs *Ocln* (Occludin), *Tjp1* (Zona occludens-1), and *F11r* (Junctional adhesion molecule A), whereas *Cldn11* (Claudin11) remained unaltered (Figure 3B).

To validate the gonadal dysfunction associated with HTN, we also examined sperm collected from the caudal portion of the epididymides for sperm concentration, motility, morphology, and various functional traits such as acrosome integrity and mitochondrial activity. Consistent with testes dysfunction, we found a significant decrease in sperm concentration in the SSHTN mice when compared with the control mice (Figure 3C). Sperm progressive motility was unaltered in the SSHTN mice (Supplementary Figure S1). The SSHTN mice also had a significantly increased percentage of sperm with abnormal morphology (Figure 3D) and damaged acrosome (Figure 3E), along with a significant decrease in the percentage of sperm with functional mitochondria (Figure 3F). We found almost identical results in a comparable model of SSHTN in which males were given L-NAME (1.5 mg/ml) for 4 weeks, followed by a tap water washout of 1 week, and then a 4% salt diet for 3 weeks [46]. This comparable method of SSHTN induction was also associated with significantly increased gonadal M1 macrophages (Supplementary Figure S2), significantly decreased M2 macrophages (Supplementary Figure S2), significantly increased gene expression of proinflammatory mediators (Supplementary Figure S3A), significantly increased gene expression of lymphatic markers and chemokines (Supplementary Figure S3B), and testicular dysfunction (Supplementary Figure S3C,D). Collectively, these results indicate that SSHTN leads to poor sperm quality and quantity by adversely affecting the expression of genes involved in the process of steroidogenesis and spermatogenesis.

Like testes, ovarian steroidogenesis is also essential for the maintenance of reproductive tissues, folliculogenesis and ovulation, and establishment of pregnancy, that are under the intricate control of the pituitary gonadotropins FSH and LH [47,48]. We investigated the effect of SSHTN on ovarian steroidogenesis and its regulation by measuring gene expression of cholesterol transport protein, key steroidogenic enzymes, and hormone receptors. Ovaries from SSHTN mice demonstrated a significantly increased expression of *Star, Hsd3b1, Cyp11a1,* and *Cyp17a1,* with a simultaneous decrease in the expression of *Cyp19a1,* the

aromatase enzyme responsible for estrogen synthesis from androgen precursors (Figure 3G). The hormone receptors *Ar*, *Fshr, Era, Erb,* and *Lhr* were increased significantly in ovaries from the SSHTN mice (Figure 3G). The expression of *Inhbb* was increased significantly, whereas *Inhba* remained unaltered in ovaries from the SSHTN mice (Figure 3G). Taken together, these results indicate that SSHTN increased the expression of steroidogenic enzymes with a simultaneous decrease in aromatase that might lead to reduced availability of estrogen and increased androgen levels in the ovarian tissue.

LHTN is associated with altered macrophages, inflammation, and increased lymphatics in both testes and ovaries

To mimic hypertensive patients with elevated levels of the endogenous nitric oxide synthase inhibitor asymmetric dimethylarginine, we administered L-NAME in the drinking water for 3 weeks as described previously [28]. We then sought to determine whether alterations in gonadal macrophages, inflammation, and inflammation-associated lymphangiogenesis also occur in this model of HTN that is independent of salt. We confirmed the development of LHTN in both male (Figure 4A) and female (Figure 4B) mice. There were no differences in body weights of male and female mice, or in the relative weight of ovaries in LHTN mice, but there was a significant increase in the relative weight of testes in LHTN mice compared with control mice (Supplementary Table S4), similar to mice with SSHTN. Using flow cytometry, we found a significant increase in both M1 and M2 macrophages in the testes of LHTN mice (Figure 4C), while ovaries exhibited a significant decrease in M1 macrophages and a significant increase in M2 (Figure 4D). Like mice with SSHTN, the expression of the proinflammatory mediators *Il1b, Il6, Il17, Tnfa, Ifng,* and *Nos2* was increased significantly in the testes of mice with LHTN (Figure 4E). Ovaries from LHTN mice had identical results with significantly increased expression of *Il1b, Il6, Il17, Tnfa, Ifng,* and *Nos2* (Figure 4F). We labeled the lymphatics with LYVE-1 staining in testis (Figure 5A) and ovary (Figure 5B) sections and confirmed a significantly increased lymphatic vessel density in LHTN mice. Gene expression analysis congruently demonstrated a significant increase in lymphatic markers (*Lyve1, Prox1, Pdpn, Vegfc*, *Vegfd*, *Vegfr2*, and *Vegfr3*), cell adhesion molecule (*Icam*), and lymphatic endothelial cell-specific chemokines (*Ccl21* and *Ccl19*) and receptor (*Ccr7*) in the testes of LHTN mice (Figure 5C). There was a significant increase in the expression of *Prox1* and *Vegfd* in ovaries from LHTN mice (Figure 5D). 3-D model and reconstruction of confocal images of testes and ovaries from LHTN mice can be observed in (Figure 5E–H) and Supplementary Videos S5 and S6, respectively. These data suggest that LHTN alters gonadal macrophages and is associated with gonadal inflammation and a compensatory increase in lymphatic density.

LHTN is associated with impaired gonadal function

We next conducted a similar study as that in SSHTN mice to examine whether LHTN is also associated with gonadal dysfunction. Gene expression analysis revealed a significant decrease in *Star, Hsd17b1,* and *Cyp17a1* in the testes of mice with LHTN, whereas *Hsd3b1* and *Cyp11a1* remained unaltered (Figure 6A). LHTN also significantly decreased the expression of *Ar, Era,* and *Lhr* in the testes of LHTN mice (Figure 6A). There was also a significant increase in the expression of *Inhba* and *Scgb1b24,* and significantly decreased expression of *Inhbb* and *Trf* in the testes of LHTN mice (Figure 6B). We

also observed a significantly decreased expression of *Cldn11* and *Tjp1* in the testes of LHTN mice (Figure 6B). Sperm collected from the caudal portion of the epididymides from LHTN mice revealed a significant decrease in sperm concentration (Figure 6C), whereas sperm motility remained unchanged (Supplementary Figure S4). There was a significantly increased percentage of sperm with abnormal morphology (Figure 6D) and damaged acrosome (Figure 6E), and a simultaneous decrease in the percentage of sperm with functional mitochondria (Figure 6F), which is congruent with that found in the SSHTN mice. Taken together, these results highlight the detrimental effect that LHTN has on the genes regulating steroidogenesis and spermatogenesis in male mice.

Ovaries from LHTN mice had significantly increased expression of *Star, Hsd17b1*, and *Cyp11a1*, along with a significant decrease in the expression of *Hsd3b1* and *Cyp17a1,* while there was no change in the expression of *Cyp19a1* (Figure 6G). There was also a significant decrease in the expression of *Erα*, whereas *Ar, Fshr, Erb,* and *Lhr* were unaltered in the ovaries from LHTN mice (Figure 6G). The gene expression of *Inhba* and *Inhbb* were increased significantly in the ovaries from LHTN mice (Figure 6G). Collectively, these results suggest that LHTN modifies the expression of genes involved in the steroidogenic pathway in the ovaries.

Discussion

HTN is strongly associated with impaired reproductive function in both men and women, however, the mechanisms involved remain obscure. To the best of our knowledge, this is the first study to demonstrate that HTN changes gonadal macrophages, and this is associated with gonadal inflammation, inflammation-associated lymphangiogenesis, and dysfunction. The current study has given a new immunological perspective at the gonadal level in hypertensive mice. We demonstrated an increase in M1 macrophages and decrease in M2 phenotype in both testes and ovaries from the SSHTN mice, which is associated with increased expression of proinflammatory mediators, an increase in lymphatics, and altered gonadal function. Subsequently, we also demonstrated that LHTN significantly increased M2 macrophages in both testes and ovaries along with a concurrent increase in M1 macrophages in testes alone. Identical with SSHTN, LHTN is also associated with gonadal inflammation, inflammation-associated lymphangiogenesis, and impaired gonadal function.

Previous study has reported hypertrophy of testis in Spontaneously Hypertensive Rats [15] that agrees with the increased relative testis weight observed in SSHTN and HTN mice in our present study. There were no significant changes in the relative weight of ovaries in the hypertensive groups.

HTN is characterized by a state of chronic low-grade inflammation with the involvement of activated innate and adaptive immunity. Macrophages are one of the most abundant heterogenous populations of immune cells involved in the inflammatory responses in HTN [21]. Testicular macrophages are involved in the maintenance of the immune privilege state of the testis, steroidogenesis, and differentiation of spermatogonia, in addition to immune surveillance [49]. Similarly, ovarian macrophages are known to stimulate cellular proliferation and follicle growth, steroidogenesis, suppress follicular apoptosis,

and regulate vascularization and tissue remodeling during different stages of the ovarian cycle [50]. Under normal conditions, the majority of testicular macrophages exhibit a M2 phenotype [51], consistent with our results in control testes. In contrast, we observed a higher proportion of M1 than M2 macrophages in control ovaries. Unfortunately, little is known about the putative phenotypes of macrophages and their functional polarization in ovaries. Studies have reported that HTN and SSHTN promotes M1 polarization in circulating monocytes and increases accumulation of M1 macrophages in the end organs like the kidney, lung, and liver [31–36]. EAO, an established model of chronic testicular inflammation, was associated with increased M1 macrophages in the testes along with increased levels of monocyte chemoattractant protein-1 (MCP-1), IL-6, and TNF [52]. Lima et al. [53] reported increased M1 macrophages in the ovaries of rats with polycystic ovary syndrome (PCOS) that also associates with low-grade chronic inflammation. Accordingly, one of the prominent observations in our study is increased M1 macrophages in both testes and ovaries from SSHTN mice and in the testes from LHTN mice, which align with results from above studies. However, the exact mechanism behind the increase in M2 macrophages observed in the testes and ovaries from LHTN is unknown. It might be due, in part, to the effect of reduced nitric oxide on macrophage physiology at the gonadal level. Nonetheless, an imbalance in gonadal M1/M2 ratio, as observed in the current study, may be one of the factors contributing to gonadal dysfunction in HTN.

Few studies have demonstrated inflammation and inflammation-associated lymphangiogenesis in reproductive tissues in certain pathological conditions [54–56]. Consistently, in the present study, we found increased gene expression of proinflammatory mediators and a compensatory increase in lymphatics in both testes and ovaries from mice with SSHTN and HTN. Systemic and local inflammation is well known to disrupt the hypothalamic–pituitary–testicular axis, inhibiting LC function and spermatogenesis [57,58]. Resident macrophages, mast cells, and SCs can produce both proinflammatory and anti-inflammatory cytokines including IL-1β, IL-6, TNF-α, IFN-γ, members of the TGF-β family, and IL-10 under physiological conditions [59]. Proinflammatory cytokines are known to promote testicular inflammation and disrupt BTB by down-regulation and delocalization of critical TJPs [60–62]. A study reported down-regulation of SC TJPs such as Claudin-11, Occludin, and TJP-1 in a model of varicocele rat testes along with decreased expression of 3β*Hsd6* and *17*β*Hsd3* when compared with normal testes [63]. It was also accompanied by increased gene expression of proinflammatory cytokines (*Tnfa*, *Il1a*, and *Il6*), a leukocyte marker (*Cd45*), and T-cell markers (*Cd3g* and *Cd3d*) in the varicocele testes [63]. The inflammatory cytokines TNFα, IL1β, and IL-6 have been reported to diminish steroidogenesis in TM3 LCs [64]. In line with these studies, we also found increased gene expression of proinflammatory mediators and, decreased expression of critical TJPs and steroidogenic pathway genes in testes indicating that HTN might disrupt spermatogenesis and steroidogenesis in mice. This is supported by our results showing poor sperm quantity and quality in the hypertensive mice.

Inhibin is a dimer of a common α subunit and either a βA (inhibin A) or βB (inhibin B) subunit [65]. Inhibin B, predominantly secreted by SCs, suppresses FSH secretion from the pituitary [66]. Activin is a homodimer of two βA (activin A) and two βB subunits (activin B). Activin A stimulates FSH secretion and regulates steroidogenesis and spermatogenesis

by influencing the development of SCs and GCs [67]. Besides these functions, activin A plays a critical role in maintaining the immune privileged state within the testis [68]. Elevated expression of activin A in the testis is associated with inflammation and disruption of spermatogenesis in animal models [52,69]. Also, IL-1β is shown to increase activin A and suppress inhibin B levels in SCs *in vitro* [70]. This agrees with the up-regulated expression of *Inhba* along with decreased expression of *Inhbb* observed in the present study in both SSHTN and LHTN models. Transferrin delivers iron to the developing GCs and is a secretory product of SCs [71]. Decreased expression of *Trf* in the testes of both SSHTN and LHTN mice may be linked to disruption of spermatogenesis, resulting in poor sperm quality and quantity as observed in the current study. ABP (Secretoglobin family 1B, member 24; *Scgb1b24*), secreted by SCs, is involved in transporting and increasing the bioavailability of androgens [72]. Previous studies have reported an association between excess ABP and increased apoptosis of pachytene spermatocyte, decreased intratesticular levels of androgens, resulting in impaired spermatogenesis in a transgenic mouse model [73,74]. The overexpression of *Scgb1b24* in the testes of hypertensive mice in the present study is consistent with these reports. Since ABP-bound androgens are considered biologically inactive [75], the decreased availability of androgens might be one of the reasons for the poor quantity and quality of sperm observed in the current study.

Low-grade, chronic inflammation and impaired folliculogenesis, and ovulation has been documented in females with obesity and PCOS [76,77]. Elevated expression of IL-1, TNF-α, and IFN-γ was observed in autoimmune ovarian disease, a chronic inflammatory disease model [78]. Endometriotic tissue exhibited inflammation-associated lymphangiogenesis in both humans and mice [54,56]. A strong correlation between hyperandrogenism and inflammation has been established in PCOS [79]. Elevated serum inhibin B levels have been reported in women with PCOS [80]. In accordance with the aforementioned studies, the data presented here suggest that in the SSHTN mice, inflammation is associated with increased lymphatics, expression of steroidogenic pathway genes and inhibin B, and a concurrent decrease in the expression of *Cyp19a1*, which might lead to hyperandrogenism and disturb normal ovarian functions.

Taken together, our explorative study was performed to gain insights into the association between gonadal macrophages and inflammation in the reproductive dysfunction observed in HTN. Although the current study is largely observational, we have established for the first time to our knowledge that altered macrophage polarization occurs in the gonads and is associated with gonadal inflammation, inflammation-associated lymphangiogenesis, and dysfunction in hypertensive animals. Studies are underway to determine if manipulation of M1 and M2 macrophages can reduce gonadal inflammation and improve gonadal function. It is possible that normalizing gonadal macrophage polarization may have beneficial effects on reproductive health in people with HTN.

Supplementary Material

Refer to Web version on PubMed Central for supplementary material.

Acknowledgements

We thank Robbie Moore and Dr. Joseph Rutkowski for the technical assistance and advice. We acknowledge the facilities provided by Integrated Microscopy & Imaging Laboratory (IMIL) and College of Medicine-Cell Analysis Facility (COM-CAF) cores at Texas A&M University, Bryan, Texas.

Funding

The present study was supported by an American Heart Association Postdoctoral Fellowship (#916912) to S.N. and National Institutes of Health RO1 (DK120493) to B.M.M.

Data Availability

All supporting data are in the paper.

Abbreviations

ABP	androgen-binding protein
Ar	androgen receptor
BTB	blood–testis barrier
BWW	Biggers-Whitten-Whittingham
CYP	cytochrome P450
DAPI	4’,6-diamidino-2-phenylindole
DPBS	Dulbecco’s phosphate-buffered saline
EAO	experimental autoimmune orchitis
Era	estrogen receptor subtype a
Erb	estrogen receptor b
FITC-PNA	fluorescent-labeled peanut agglutinin
FMO	fluorescence minus one
FSH	follicle-stimulating hormone
GC	germ cell
HTN	hypertension
HSD	hydroxysteroid dehydrogenases
Inhbb	Inhibin B
L-NAME	nitro-l-arginine methyl ester hydrochloride
LC	Leydig cell
LH	luteinizing hormone

LHTN	L-NAME-induced hypertension
LYVE-1	lymphatic vessel endothelial hyaluronan receptor 1
M1	proinflammatory macrophages
M2	anti-inflammatory macrophages
MCP-1	monocyte chemoattractant protein-1
MIP-1	macrophage inflammatory protein-1
PBS	phosphate-buffered saline
PCOS	polycystic ovarian syndrome
Pdpn	podoplanin
PFA	paraformaldehyde
Prox1	a lymphatic endothelial cell transcription factor
Rh123	rhodamine123
SBP	systolic blood pressure
SC	Sertoli cell
SEM	standard error of the mean
SSHTN	salt-sensitive hypertension
StAR	steroidogenic acute regulatory protein
T	testosterone
TJ	tight junction
TJP	tight junction proteins
Trf	transferrin
VEGF-C	vascular endothelial growth factor C
VEGF-D	vascular endothelial growth factor D
VEGFR-3	vascular endothelial growth factor receptor 3

References

1. Mozaffarian D, Benjamin EJ, Go AS, Arnett DK, Blaha MJ, Cushman M et al. (2015) Heart disease and stroke statistics–2015 update: a report from the American Heart Association. Circulation 131, e29–e322 [PubMed: 25520374]
2. Whelton PK, Carey RM, Aronow WS, Casey DE Jr., Collins KJ, Dennison Himmelfarb C et al. (2018) 2017 ACC/AHA/AAPA/ABC/ACPM/AGS/APhA/ASH/ASPC/NMA/PCNA guideline for the prevention, detection, evaluation, and management of high blood pressure in adults: executive summary: a report of the American College of Cardiology/American Heart Association Task Force

on Clinical Practice Guidelines. Hypertension 71, 1269–1324, 10.1161/HYP.0000000000000066 [PubMed: 29133354]

3. Xie X, Atkins E, Lv J, Bennett A, Neal B, Ninomiya T et al. (2016) Effects of intensive blood pressure lowering on cardiovascular and renal outcomes: updated systematic review and meta-analysis. Lancet 387, 435–443, 10.1016/S0140-6736(15)00805-3 [PubMed: 26559744]
4. Navaneethabalakrishnan S, Goodlett BL, Lopez AH, Rutkowski JM and Mitchell BM (2020) Hypertension and reproductive dysfunction: a possible role of inflammation and inflammation-associated lymphangiogenesis in gonads. Clin. Sci. (Lond.) 134, 3237–3257, 10.1042/CS20201023 [PubMed: 33346358]
5. Aranda P, Ruilope LM, Calvo C, Luque M, Coca A and Gil de Miguel A (2004) Erectile dysfunction in essential arterial hypertension and effects of sildenafil: results of a Spanish national study. Am. J. Hypertens 17, 139–145, 10.1016/j.amjhyper.2003.09.006 [PubMed: 14751656]
6. Guo D, Li S, Behr B and Eisenberg ML (2017) Hypertension and male fertility. World J. Mens. Health 35, 59–64, 10.5534/wjmh.2017.35.2.59 [PubMed: 28868816]
7. Foy CG, Newman JC, Berlowitz DR, Russell LP, Kimmel PL, Wadley VG et al. (2019) Blood pressure, sexual activity, and erectile function in hypertensive men: baseline findings from the Systolic Blood Pressure Intervention Trial (SPRINT). J. Sex Med 16, 235–247, 10.1016/j.jsxm.2018.12.007 [PubMed: 30655182]
8. Duncan LE, Lewis C, Jenkins P and Pearson TA (2000) Does hypertension and its pharmacotherapy affect the quality of sexual function in women? Am. J. Hypertens 13, 640–647, 10.1016/S0895-7061(99)00288-5 [PubMed: 10912747]
9. Doumas M, Tsiodras S, Tsakiris A, Douma S, Chounta A, Papadopoulos A et al. (2006) Female sexual dysfunction in essential hypertension: a common problem being uncovered. J. Hypertens 24, 2387–2392, 10.1097/01.hjh.0000251898.40002.5b [PubMed: 17082720]
10. Bramham K, Parnell B, Nelson-Piercy C, Seed PT, Poston L and Chappell LC (2014) Chronic hypertension and pregnancy outcomes: systematic review and meta-analysis. BMJ 348, g2301, 10.1136/bmj.g2301 [PubMed: 24735917]
11. Akagashi K, Itoh N, Kumamoto Y, Tsukamoto T, Suzuki T and Ohta Y (1996) Hypertensive changes in intratesticular arteries impair spermatogenesis of the stroke-prone spontaneously hypertensive rat. J. Androl 17, 367–374 [PubMed: 8889699]
12. Breigeiron MK, Lucion AB and Sanvitto GL (2007) Effects of renovascular hypertension on reproductive function in male rats. Life Sci. 80, 1627–1634, 10.1016/j.lfs.2007.01.030 [PubMed: 17316702]
13. Ribeiro RA, Raineki C, Gonçalves O, Franci CR, Lucion AB and Sanvitto GL (2013) Reproductive dysfunction in female rats with renovascular hypertension. Am. J. Hypertens 26, 104–110, 10.1093/ajh/hps026 [PubMed: 23382333]
14. Yeasmin N, Akhter QS, Mahmuda S, Banu N, Yeasmin S, Akhter S et al. (2017) Association of hypertension with serum estrogen level in postmenopausal women. Mymensingh Med. J 26, 635–641 [PubMed: 28919621]
15. Colli LG, Belardin LB, Echem C, Akamine EH, Antoniassi MP, Andretta RR et al. (2019) Systemic arterial hypertension leads to decreased semen quality and alterations in the testicular microcirculation in rats. Sci. Rep 9, 11047, 10.1038/s41598-019-47157-w [PubMed: 31363128]
16. Chae CU, Lee RT, Rifai N and Ridker PM (2001) Blood pressure and inflammation in apparently healthy men. Hypertension 38, 399–403, 10.1161/01.HYP.38.3.399 [PubMed: 11566912]
17. De Ciuceis C, Amiri F, Brassard P, Endemann DH, Touyz RM and Schiffrin EL (2005) Reduced vascular remodeling, endothelial dysfunction, and oxidative stress in resistance arteries of angiotensin II-infused macrophage colony-stimulating factor-deficient mice: evidence for a role in inflammation in angiotensin-induced vascular injury. Arterioscler. Thromb. Vasc. Biol 25, 2106–2113, 10.1161/01.ATV.0000181743.28028.57 [PubMed: 16100037]
18. Guzik TJ, Hoch NE, Brown KA, McCann LA, Rahman A, Dikalov S et al. (2007) Role of the T cell in the genesis of angiotensin II induced hypertension and vascular dysfunction. J. Exp. Med 204, 2449–2460, 10.1084/jem.20070657 [PubMed: 17875676]

19. Youn JC, Yu HT, Lim BJ, Koh MJ, Lee J, Chang DY et al. (2013) Immunosenescent CD8+ T cells and C-X-C chemokine receptor type 3 chemokines are increased in human hypertension. Hypertension 62, 126–133, 10.1161/HYPERTENSI0NAHA.113.00689 [PubMed: 23716586]
20. Mian MO, Barhoumi T, Briet M, Paradis P and Schiffrin EL (2016) Deficiency of T-regulatory cells exaggerates angiotensin II-induced microvascular injury by enhancing immune responses. J. Hypertens 34, 97–108, 10.1097/HJH.0000000000000761 [PubMed: 26630215]
21. Caillon A and Schiffrin EL (2016) Role of inflammation and immunity in hypertension: recent epidemiological, laboratory, and clinical evidence. Curr. Hypertens. Rep 18, 21, 10.1007/s11906-016-0628-7 [PubMed: 26846785]
22. Ko EA, Amiri F, Pandey NR, Javeshghani D, Leibovitz E, Touyz RM et al. (2007) Resistance artery remodeling in deoxycorticosterone acetate-salt hypertension is dependent on vascular inflammation: evidence from m-CSF-deficient mice. Am. J. Physiol. Heart Circ. Physiol 292, H1789–H1795, 10.1152/ajpheart.01118.2006 [PubMed: 17142347]
23. Wenzel P, Knorr M, Kossmann S, Stratmann J, Hausding M, Schuhmacher S et al. (2011) Lysozyme M-positive monocytes mediate angiotensin II-induced arterial hypertension and vascular dysfunction. Circulation 124, 1370–1381, 10.1161/CIRCULATI0NAHA.111.034470 [PubMed: 21875910]
24. Crowley SD, Song YS, Lin EE, Griffiths R, Kim HS and Ruiz P (2010) Lymphocyte responses exacerbate angiotensin II-dependent hypertension. Am. J. Physiol. Regul. Integr. Comp. Physiol 298, R1089–R1097, 10.1152/ajpregu.00373.2009 [PubMed: 20147609]
25. De Miguel C, Das S, Lund H and Mattson DL (2010) T lymphocytes mediate hypertension and kidney damage in Dahl salt-sensitive rats. Am. J. Physiol. Regul. Integr. Comp. Physiol 298, R1136–R1142, 10.1152/ajpregu.00298.2009 [PubMed: 20147611]
26. Itani HA, Xiao L, Saleh MA, Wu J, Pilkinton MA, Dale BL et al. (2016) CD70 exacerbates blood pressure elevation and renal damage in response to repeated hypertensive stimuli. Circ. Res 118, 1233–1243, 10.1161/CIRCRESAHA.115.308111 [PubMed: 26988069]
27. Norlander AE, Saleh MA, Kamat NV, Ko B, Gnecco J, Zhu L et al. (2016) Interleukin-17A regulates renal sodium transporters and renal injury in angiotensin II-induced hypertension. Hypertension 68, 167–174, 10.1161/HYPERTENSI0NAHA.116.07493 [PubMed: 27141060]
28. Lopez Gelston CA, Balasubbramanian D, Abouelkheir GR, Lopez AH, Hudson KR, Johnson ER et al. (2018) Enhancing renal lymphatic expansion prevents hypertension in mice. Circ. Res 122, 1094–1101, 10.1161/CIRCRESAHA.118.312765 [PubMed: 29475981]
29. Balasubbramanian D, Gelston CAL, Lopez AH, Iskander G, Tate W, Holderness H et al. (2020) Augmenting renal lymphatic density prevents angiotensin II-induced hypertension in male and female mice. Am. J. Hypertens 33, 61–69, 10.1093/ajh/hpz139 [PubMed: 31429865]
30. Mosser DM and Edwards JP (2008) Exploring the full spectrum of macrophage activation. Nat. Rev. Immunol 8, 958–969, 10.1038/nri2448 [PubMed: 19029990]
31. Ndisang JF and Mishra M (2013) The heme oxygenase system selectively suppresses the proinflammatory macrophage m1 phenotype and potentiates insulin signaling in spontaneously hypertensive rats. Am. J. Hypertens 26, 1123–1131, 10.1093/ajh/hpt082 [PubMed: 23757400]
32. Gomolak JR and Didion SP (2014) Angiotensin II-induced endothelial dysfunction is temporally linked with increases in interleukin-6 and vascular macrophage accumulation. Front. Physiol 5, 396, 10.3389/fphys.2014.00396 [PubMed: 25400581]
33. Harwani SC, Ratcliff J, Sutterwala FS, Ballas ZK, Meyerholz DK, Chapleau MW et al. (2016) Nicotine Mediates CD161a+ Renal Macrophage Infiltration and Premature Hypertension in the Spontaneously Hypertensive Rat. Circ. Res 119, 1101–1115, 10.1161/CIRCRESAHA.116.309402 [PubMed: 27660287]
34. Martín-Fernández B, Rubio-Navarro A, Cortegano I, Ballesteros S, Alía M, Cannata-Ortiz P et al. (2016) Aldosterone induces renal fibrosis and inflammatory M1-macrophage subtype via mineralocorticoid receptor in rats. PloS ONE 11, e0145946, 10.1371/journal.pone.0145946 [PubMed: 26730742]
35. Fehrenbach DJ, Abais-Battad JM, Dasinger JH, Lund H and Mattson DL (2019) Salt-sensitive increase in macrophages in the kidneys of Dahl SS rats. Am. J. Physiol. Renal. Physiol 317, F361–F374, 10.1152/ajprenal.00096.2019 [PubMed: 31215801]

36. Zawia A, Arnold ND, West L, Pickworth JA, Turton H, Iremonger J et al. (2021) Altered macrophage polarization induces experimental pulmonary hypertension and is observed in patients with pulmonary arterial hypertension. Arterioscler. Thromb. Vasc. Biol 41, 430–445 [PubMed: 33147993]
37. Tsetsarkin KA, Acklin JA, Liu G, Kenney H, Teterina NL, Pletnev AG et al. (2020) Zika virus tropism during early infection of the testicular interstitium and its role in viral pathogenesis in the testes. PLoS Pathog. 16, e1008601, 10.1371/journal.ppat.1008601 [PubMed: 32614902]
38. Ono Y, Nagai M, Yoshino O, Koga K, Nawaz A, Hatta H et al. (2018) CD11c+ M1-like macrophages (MΦs) but not CD206+ M2-like MΦ are involved in folliculogenesis in mice ovary. Sci. Rep 8, 8171, 10.1038/s41598-018-25837-3 [PubMed: 29802255]
39. Hasegawa S, Susaki EA, Tanaka T, Komaba H, Wada T, Fukagawa M et al. (2019) Comprehensive three-dimensional analysis (CUBIC-kidney) visualizes abnormal renal sympathetic nerves after ischemia/reperfusion injury. Kidney Int. 96, 129–138, 10.1016/j.kint.2019.02.011 [PubMed: 30979565]
40. O'Donnell L, Stanton P and de Kretser DM (2017) Endocrinology of the male reproductive system and spermatogenesis. In Endocrinology of Male Reproduction (Feingold KR, Anawalt B, Boyce A and McLachlan RI, eds), pp. 1–69
41. Smith LB and Walker WH (2014) The regulation of spermatogenesis by androgens. Semin. Cell Dev. Biol 30, 2–13, 10.1016/j.semcdb.2014.02.012 [PubMed: 24598768]
42. Miller WL and Auchus RJ (2011) The molecular biology, biochemistry, and physiology of human steroidogenesis and its disorders. Endocr. Rev 32, 81–151, 10.1210/er.2010-0013 [PubMed: 21051590]
43. Su W, Mruk DD and Cheng CY (2013) Regulation of actin dynamics and protein trafficking during spermatogenesis–insights into a complex process. Crit. Rev. Biochem. Mol. Biol 48, 153–172, 10.3109/10409238.2012.758084 [PubMed: 23339542]
44. Kaitu'u-Lino TJ, Sluka P, Foo CF and Stanton PG (2007) Claudin-11 expression and localisation is regulated by androgens in rat Sertoli cells in vitro. Reproduction 133, 1169–1179, 10.1530/REP-06-0385 [PubMed: 17636171]
45. Tarulli GA, Meachem SJ, Schlatt S and Stanton PG (2008) Regulation of testicular tight junctions by gonadotrophins in the adult Djungarian hamster in vivo. Reproduction 135, 867–877, 10.1530/REP-07-0572 [PubMed: 18502899]
46. Giani JF, Bernstein KE, Janjulia T, Han J, Toblli JE, Shen XZ et al. (2015) Salt sensitivity in response to renal injury requires renal angiotensin-converting enzyme. Hypertension 66, 534–542, 10.1161/HYPERTENSIONAHA.115.05320 [PubMed: 26150439]
47. Drummond AE (2006) The role of steroids in follicular growth. Reprod. Biol. Endocrinol 4, 16, 10.1186/1477-7827-4-16 [PubMed: 16603089]
48. Lapointe E and Boerboom D (2011) WNT signaling and the regulation of ovarian steroidogenesis. Front. Biosci. (Schol Ed.) 3, 276–285 [PubMed: 21196376]
49. Bhushan S, Theas MS, Guazzone VA, Jacobo P, Wang M, Fijak M et al. (2020) Immune cell subtypes and their function in the testis. Front. Immunol 11, 583304, 10.3389/fimmu.2020.583304 [PubMed: 33101311]
50. Zhang Z, Huang L and Brayboy L (2021) Macrophages: an indispensable piece of ovarian health. Biol. Reprod 104, 527–538, 10.1093/biolre/ioaa219 [PubMed: 33274732]
51. Bhushan S, Tchatalbachev S, Lu Y, Fröhlich S, Fijak M, Vijayan V et al. (2015) Differential activation of inflammatory pathways in testicular macrophages provides a rationale for their subdued inflammatory capacity. J. Immunol 194, 5455–5464, 10.4049/jimmunol.1401132 [PubMed: 25917085]
52. Nicolas N, Michel V, Bhushan S, Wahle E, Hayward S, Ludlow H et al. (2017) Testicular activin and follistatin levels are elevated during the course of experimental autoimmune epididymo-orchitis in mice. Sci. Rep. 7, 42391, 10.1038/srep42391 [PubMed: 28205525]
53. Lima PDA, Nivet AL, Wang Q, Chen YA, Leader A, Cheung A et al. (2018) Polycystic ovary syndrome: possible involvement of androgen-induced, chemerin-mediated ovarian recruitment of monocytes/macrophages. Biol. Reprod 99, 838–852, 10.1093/biolre/ioy096 [PubMed: 29688269]

54. Reichelt U, Keichel S, Barcena de Arellano ML, Chiantera V, Schneider A and Mechsner S (2012) High lymph vessel density and expression of lymphatic growth factors in peritoneal endometriosis. Reprod. Sci 19, 876–882, 10.1177/1933719112438440 [PubMed: 22539358]
55. Hirai S, Naito M, Terayama H, Qu N, Kuerban M, Musha M et al. (2013) Lymphangiogenesis in chronic inflammation in the testis. Andrology 1, 147–154, 10.1111/j.2047-2927.2012.00015.x [PubMed: 23258644]
56. Hattori K, Ito Y, Honda M, Sekiguchi K, Hosono K, Shibuya M et al. (2020) Lymphangiogenesis induced by vascular endothelial growth factor receptor 1 signaling contributes to the progression of endometriosis in mice. J. Pharmacol. Sci 143, 255–263, 10.1016/j.jphs.2020.05.003 [PubMed: 32487450]
57. O'Bryan MK, Schlatt S, Phillips DJ, de Kretser DM and Hedger MP (2000) Bacterial lipopolysaccharide-induced inflammation compromises testicular function at multiple levels in vivo. Endocrinology 141, 238–246, 10.1210/endo.141.1.7240 [PubMed: 10614644]
58. Hales DB (2002) Testicular macrophage modulation of Leydig cell steroidogenesis. J. Reprod. Immunol 57, 3–18, 10.1016/S0165-0378(02)00020-7 [PubMed: 12385830]
59. O'Bryan MK, Gerdprasert O, Nikolic-Paterson DJ, Meinhardt A, Muir JA, Foulds LM et al. (2005) Cytokine profiles in the testes of rats treated with lipopolysaccharide reveal localized suppression of inflammatory responses. Am. J. Physiol. Regul. Integr. Comp. Physiol 288, R1744–R1755, 10.1152/ajpregu.00651.2004 [PubMed: 15661966]
60. Li MW, Xia W, Mruk DD, Wang CQ, Yan HH, Siu MK et al. (2006) Tumor necrosis factor {alpha} reversibly disrupts the blood-testis barrier and impairs Sertoli-germ cell adhesion in the seminiferous epithelium of adult rat testes. J. Endocrinol 190, 313–329, 10.1677/joe.1.06781 [PubMed: 16899565]
61. Pérez CV, Sobarzo CM, Jacobo PV, Pellizzari EH, Cigorraga SB, Denduchis B et al. (2012) Loss of occludin expression and impairment of blood-testis barrier permeability in rats with autoimmune orchitis: effect of interleukin 6 on Sertoli cell tight junctions. Biol. Reprod 87, 122, 10.1095/biolreprod.112.101709 [PubMed: 23018187]
62. Pèrez CV, Pellizzari EH, Cigorraga SB, Galardo MN, Naito M, Lustig L et al. (2014) IL17A impairs blood-testis barrier integrity and induces testicular inflammation. Cell Tissue Res. 358, 885–898, 10.1007/s00441-014-1995-5 [PubMed: 25231257]
63. Oh YS, Jo NH, Park JK and Gye MC (2016) Changes in inflammatory cytokines accompany deregulation of claudin-11, resulting in inter-sertoli tight junctions in varicocele rat testes. J. Urol 196, 1303–1312, 10.1016/j.juro.2016.05.004 [PubMed: 27164517]
64. Leisegang K and Henkel R (2018) The in vitro modulation of steroidogenesis by inflammatory cytokines and insulin in TM3 Leydig cells. Reprod. Biol. Endocrinol 16, 26, 10.1186/s12958-018-0341-2 [PubMed: 29566712]
65. Hayes FJ, Hall JE, Boepple PA and Crowley WF Jr. (1998) Clinical review 96: Differential control of gonadotropin secretion in the human: endocrine role of inhibin. J. Clin. Endocrinol. Metab 83, 1835–1841 [PubMed: 9626105]
66. O'Connor AE and De Kretser DM (2004) Inhibins in normal male physiology. Semin. Reprod. Med 22, 177–185, 10.1055/s-2004-831893 [PubMed: 15319820]
67. Mendis SH, Meachem SJ, Sarraj MA and Loveland KL (2011) Activin A balances Sertoli and germ cell proliferation in the fetal mouse testis. Biol. Reprod 84, 379–391, 10.1095/biolreprod.110.086231 [PubMed: 20926807]
68. Hedger MP and Winnall WR (2012) Regulation of activin and inhibin in the adult testis and the evidence for functional roles in spermatogenesis and immunoregulation. Mol. Cell. Endocrinol 359, 30–42, 10.1016/j.mce.2011.09.031 [PubMed: 21964464]
69. Tanimoto Y, Tanimoto K, Sugiyama F, Horiguchi H, Murakami K, Yagami K et al. (1999) Male sterility in transgenic mice expressing activin betaA subunit gene in testis. Biochem. Biophys. Res. Commun 259, 699–705, 10.1006/bbrc.1999.0833 [PubMed: 10364482]
70. Okuma Y, O'Connor AE, Muir JA, Stanton PG, de Kretser DM and Hedger MP (2005) Regulation of activin A and inhibin B secretion by inflammatory mediators in adult rat Sertoli cell cultures. J. Endocrinol 187, 125–134, 10.1677/joe.1.06266 [PubMed: 16214948]

71. Leichtmann-Bardoogo Y, Cohen LA, Weiss A, Marohn B, Schubert S, Meinhardt A et al. (2012) Compartmentalization and regulation of iron metabolism proteins protect male germ cells from iron overload. Am. J. Physiol. Endocrinol. Metab 302, E1519–E1530, 10.1152/ajpendo.00007.2012 [PubMed: 22496346]

72. Herbert Z, Weigel S, Sendemir E, Marshall A, Caldwell JD, Petrusz P et al. (2005) Androgen-binding protein is co-expressed with oxytocin in the male reproductive tract. Anat. Histol. Embryol 34, 286–293, 10.1111/j.1439-0264.2005.00605.x [PubMed: 16159369]

73. Selva DM, Tirado OM, Toràn N, Suárez-Quian CA, Reventós J and Munell F (2000) Meiotic arrest and germ cell apoptosis in androgen-binding protein transgenic mice. Endocrinology 141, 1168–1177, 10.1210/endo.141.3J383 [PubMed: 10698194]

74. Jeyaraj DA, Grossman G and Petrusz P (2005) Altered bioavailability of testosterone in androgen-binding protein-transgenic mice. Steroids 70, 704–714, 10.1016/j.steroids.2005.03.015 [PubMed: 15939447]

75. Mendel CM (1989) The free hormone hypothesis: a physiologically based mathematical model. Endocr. Rev 10, 232–274, 10.1210/edrv-10-3-232 [PubMed: 2673754]

76. Robker RL, Wu LL and Yang X (2011) Inflammatory pathways linking obesity and ovarian dysfunction. J. Reprod. Immunol 88, 142–148, 10.1016/j.jri.2011.01.008 [PubMed: 21333359]

77. Duleba AJ and Dokras A (2012) Is PCOS an inflammatory process? Fertil. Steril 97, 7–12, 10.1016/j.fertnstert.2011.11.023 [PubMed: 22192135]

78. Bagavant H, Adams S, Terranova P, Chang A, Kraemer FW, Lou Y et al. (1999) Autoimmune ovarian inflammation triggered by proinflammatory (Th1)T cells is compatible with normal ovarian function in mice. Biol. Reprod 61, 635–642, 10.1095/biolreprod61.3.635 [PubMed: 10456839]

79. Rudnicka E, Suchta K, Grymowicz M, Calik-Ksepka A, Smolarczyk K, Duszewska AM et al. (2021) Chronic low grade inflammation in pathogenesis of PCOS. Int. J. Mol. Sci 22, 10.3390/ijms22073789

80. Anderson RA, Groome NP and Baird DT (1998) Inhibin A and inhibin B in women with polycystic ovarian syndrome during treatment with FSH to induce mono-ovulation. Clin. Endocrinol. (Oxf) 48, 577–584, 10.1046/j.1365-2265.1998.00442.x [PubMed: 9666869]

Clinical perspectives

- HTN has been implicated in impaired reproductive health in both men and women. The underlying mechanisms have been largely confined to hormonal imbalance and modified vasculature in reproductive tissues.
- We observed an imbalance in macrophage polarization in both testes and ovaries of mice from two different models of HTN, SSHTN, and nitric oxide synthase inhibition-induced HTN. This altered gonadal macrophage polarization was associated with gonadal inflammation, inflammation-associated lymphangiogenesis, and dysfunction.
- The current study lays the groundwork for interventional studies to manipulate macrophage polarization, thereby providing a new therapeutic strategy to improve reproductive health in hypertensive patients.

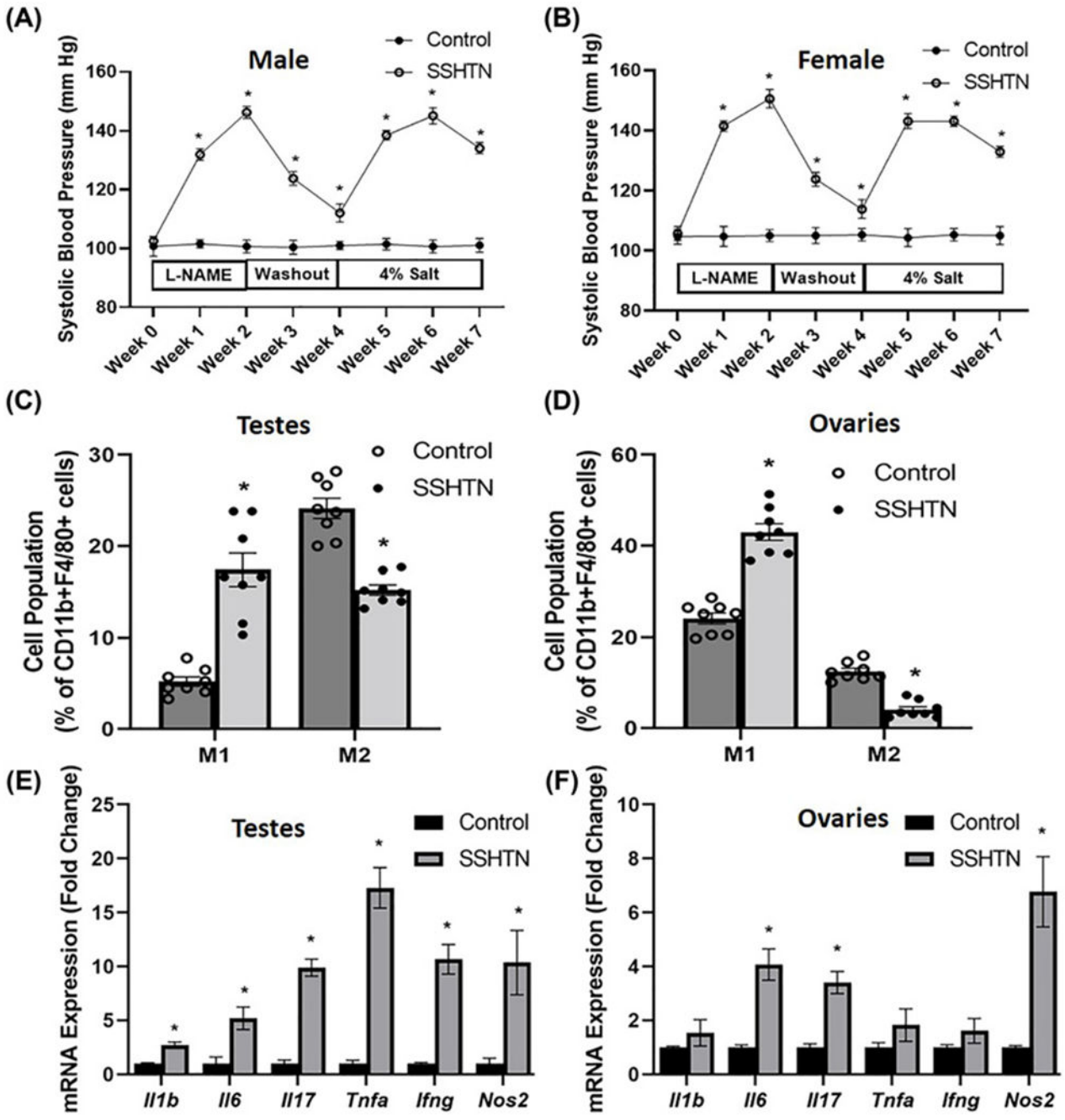

Figure 1. SSHTN mice had increased M1 macrophages, decreased M2 macrophages, and inflammation in the gonads

SBP measures in (**A**) male and (**B**) female control and mice administered L-NAME in the drinking water for 2 weeks, then 2 weeks of tap water washout, and then 3 weeks of 4% salt diet (SSHTN) (n=6 in both males and females). Macrophage (M1 and M2) populations expressed as percentage of $CD11b^{+}F4/80^{+}$ cells in (**C**) testes and (**D**) ovaries from control and SSHTN mice, as determined by flow cytometry (n=8 in both males and females). Gene expression of proinflammatory mediators in (**E**) testes and (**F**) ovaries from control and

SSHTN mice (n=6 in both males and females). Results are expressed as mean ± SEM, and statistical analysis consisted of a Student's t test. *P<0.05 vs control.

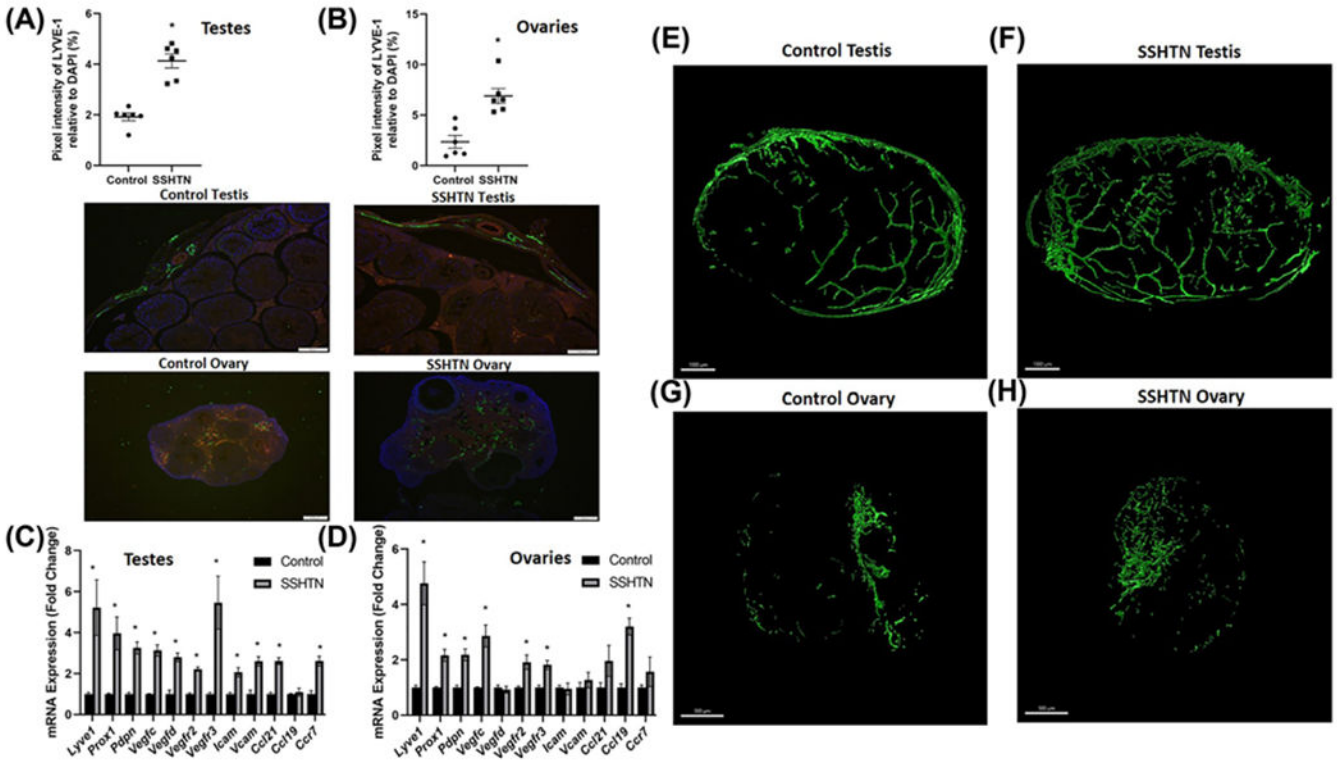

Figure 2. SSHTN increased lymphatic vessel density in the gonads

Lymphatic vessel density in (**A**) testes and (**B**) ovaries from control and SSHTN mice as determined by LYVE-1+ pixels relative to DAPI per field. Representative images of LYVE-1 immunofluorescence in testis (scale bar = 100 μm) and ovary (scale bar = 200 μm) sections (n=6 in both males and females). Green: LYVE-1; Red: CD31; Blue: DAPI. Gene expression of lymphatic vessel markers in (**C**) testes and (**D**) ovaries from the control and SSHTN mice (n=6 in both males and females). Results are expressed as mean ± SEM, and statistical analyses consisted of Student's t test. *P<0.05 vs control. Representative 3-D model of confocal images of clear, unobstructed brain/body imaging cocktails and computational analysis (CUBIC) cleared testis immunostained with LYVE-1 from (**E**) control and (**F**) SSHTN mice, n=3. Representative 3-D model of confocal images of clear, unobstructed brain/body imaging cocktails and computational analysis (CUBIC) cleared ovary immunostained with LYVE-1 from (**G**) the control and (**H**) SSHTN mice, n=3. Scale bars = 1000 μm (testis) and 500 μm (ovary).

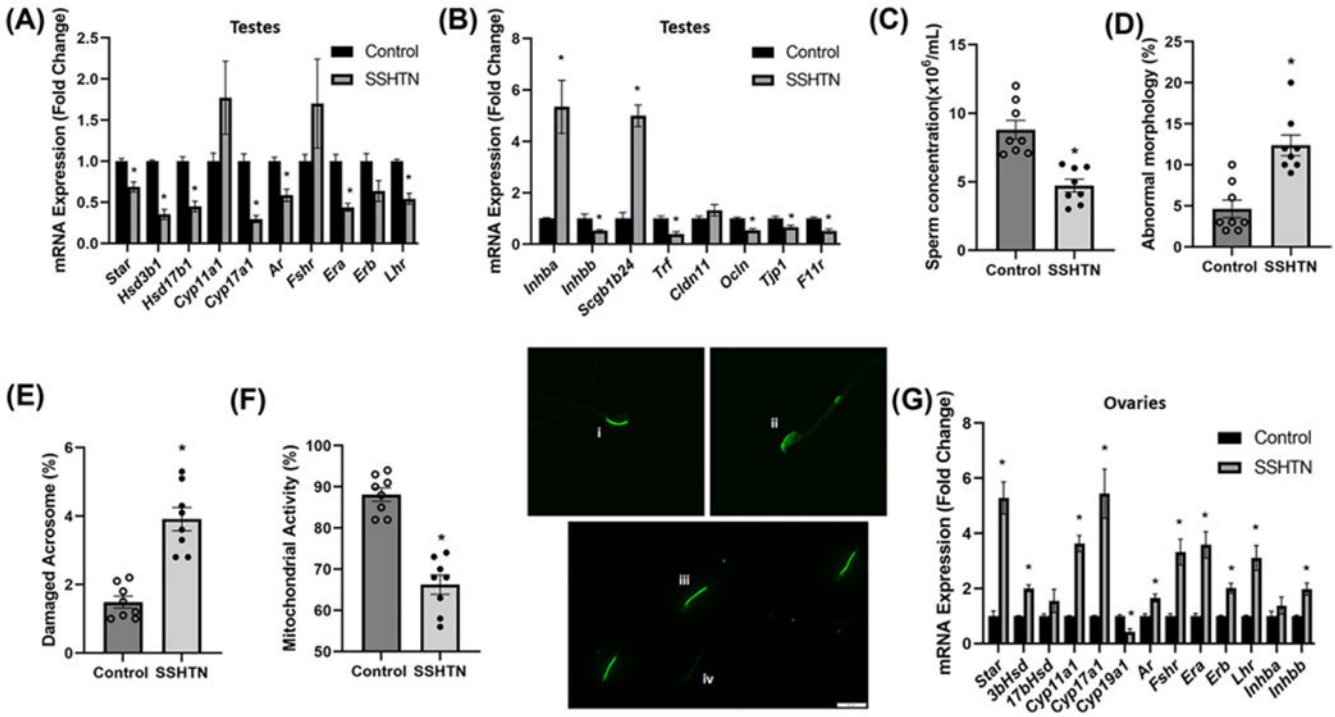

Figure 3. SSHTN mice exhibited gonadal dysfunction

Gene expression of steroidogenic pathway genes and hormone receptors in (**A**) testes from control and mice-administered L-NAME in the drinking water for 2 weeks, then 2 weeks of washout, and then a subsequent 3 weeks of 4% salt diet (SSHTN), n=6. Gene expression of secretory proteins and tight junction proteins in (**B**) testes from control and SSHTN mice, n=6. Sperm functional tests in control and SSHTN mice demonstrate (**C**) decreased sperm concentration, n=8, (**D**) increased percentage of sperm with abnormal morphology, n=8, (**E**) increased percentage of sperm with damaged acrosome, n=8, and (**F**) increased number of sperm with nonfunctional mitochondrial activity n=8. Representative images of (**i**) intact and (**ii**) damaged acrosome integrity were assessed using FITC-PNA that binds exclusively to the outer membrane of the acrosome. Scale bars = 10 μm. Florescent dye Rh123 (Rhodamine123) distinguishes (**iii**) functional and (**iv**) nonfunctional sperm mitochondria as only live cells can retain the stain after washing. Scale bars = 20 μm. Expression of steroidogenic pathway genes, hormone receptors, and secretory proteins in (**G**) ovaries from control and SSHTN mice, n=6. Results are expressed as mean ± SEM, and statistical analysis consisted of a Student's t test. *P<0.05 vs control.

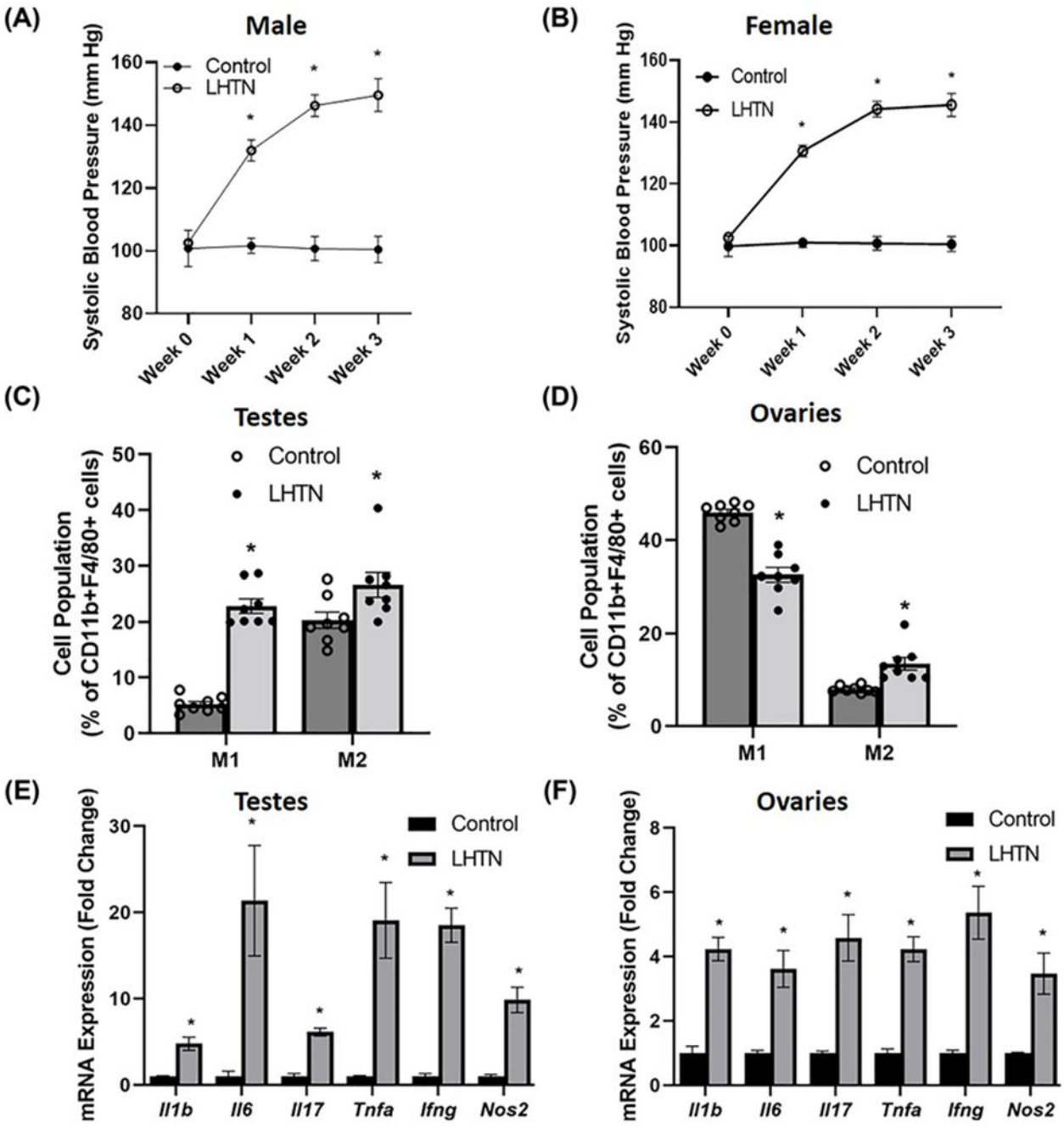

Figure 4. LHTN was associated with altered macrophage polarization and inflammation in the gonads

SBP measures in (**A**) male and (**B**) female control and mice administered L-NAME in the drinking water for 3 weeks (LHTN) (n=6 in both males and females). Macrophage (M1 and M2) populations expressed as percentage of $CD11b^{+}F4/80^{+}$ cells in (**C**) testes and (**D**) ovaries from control and LHTN mice, as measured by flow cytometry (n=8 in both males and females). Gene expression of proinflammatory mediators in (**E**) testes and (**F**) ovaries

from control and LHTN mice (n=6 in both males and females). Results are expressed as mean ± SEM, and statistical analyses consisted of Student's t test. *P<0.05 vs control.

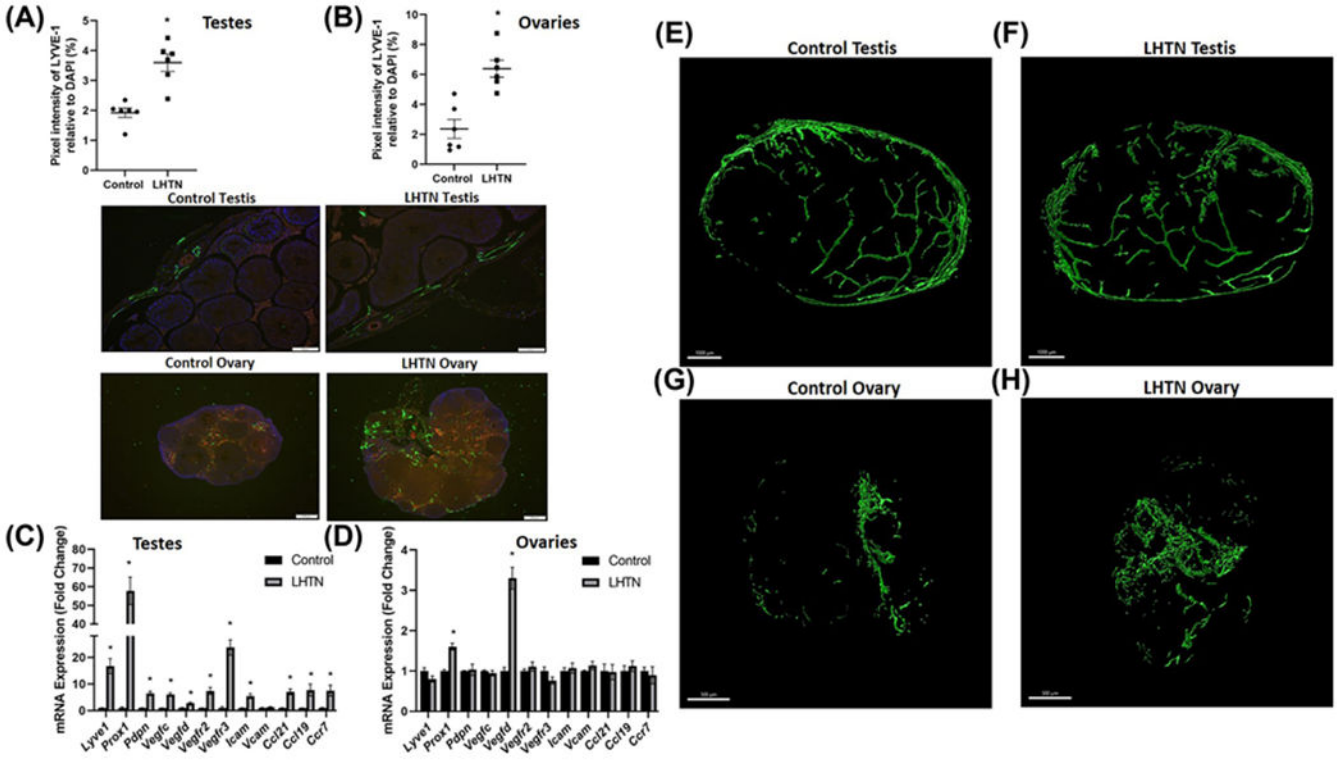

Figure 5. LHTN increased lymphatic vessel density in the gonads

Lymphatic vessel density in (**A**) testes and (**B**) ovaries from the control and LHTN mice as determined by LYVE-1+ pixels relative to DAPI per field (n=6 in both males and females). Representative images of LYVE-1 immunofluorescence in testis (scale bar = 100 μm) and ovary (scale bar = 200 μm) sections. Green: LYVE-1; Red: CD31; Blue: DAPI. Gene expression of lymphatic vessel markers in (**C**) testes and (**D**) ovaries from the control and LHTN mice (n=6 in both males and females). Results are expressed as mean ± SEM, and statistical analyses consisted of Student's t test. *P<0.05 vs control. Representative 3-D model of confocal images of clear, unobstructed brain/body imaging cocktails and computational analysis (CUBIC) cleared testis immunostained with LYVE-1 from (**E**) the control and (**F**) LHTN mice, n=3. Representative 3-D model of confocal images of clear, unobstructed brain/body imaging cocktails and computational analysis (CUBIC) cleared ovary immunostained with LYVE-1 from (**G**) the control and (**H**) LHTN mice, n=3. Scale bars = 1000 μm (testis) and 500 μm (ovary).

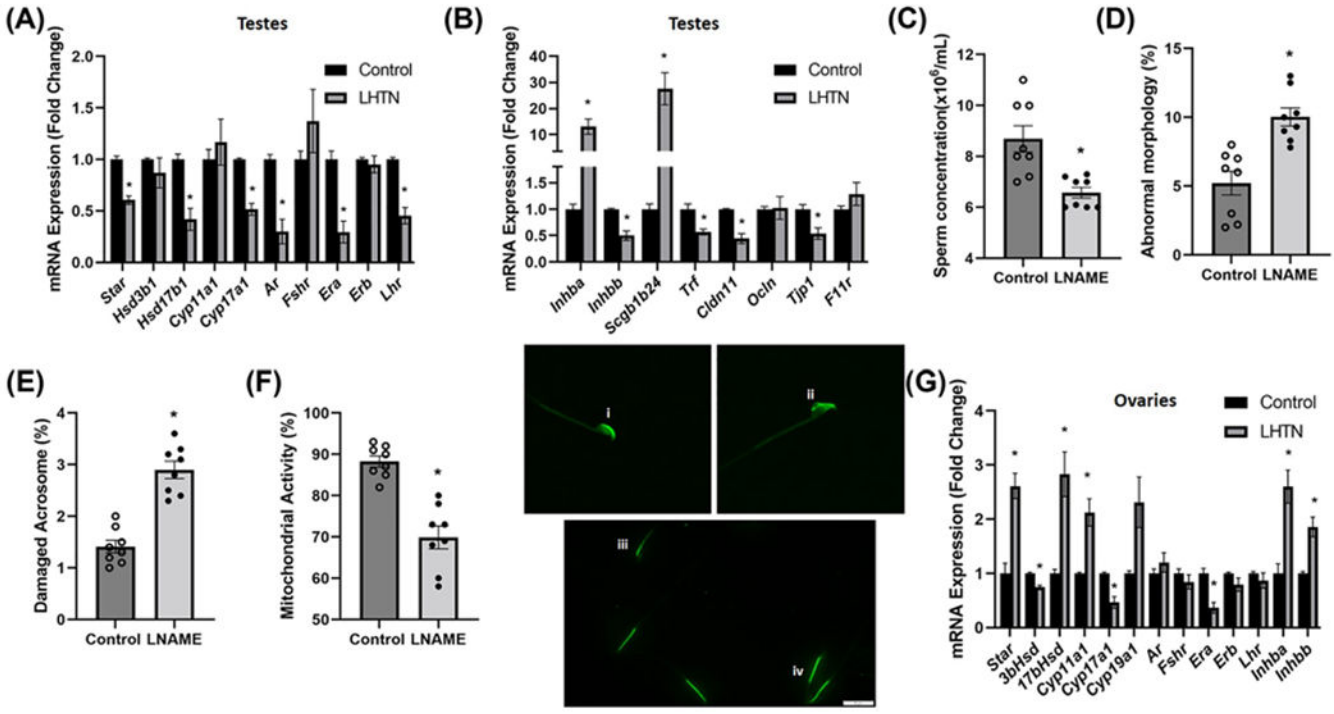

Figure 6. LHTN mice exhibited gonadal dysfunction

Gene expression of steroidogenic pathway genes and hormone receptors in (**A**) testes from the control and mice administered L-NAME in the drinking water for 3 weeks (LHTN), n=6. Gene expression of secretory proteins and tight junction proteins in (**B**) testes from the control and LHTN mice, n=6. Sperm functional tests in the control and LHTN mice demonstrate (**C**) decreased sperm concentration, n=8, (**D**) increased percentage of sperm with abnormal morphology, n=8, (**E**) increased percentage of sperm with damaged acrosome, n=8, and (**F**) increased number of sperm with nonfunctional mitochondrial activity, n=8. Representative images of (i) intact and (ii) damaged acrosome integrity were assessed using FITC-PNA that binds exclusively to the outer membrane of the acrosome. Scale bars = 10 μm. Florescent dye Rh123 (Rhodamine123) distinguishes (iii) nonfunctional and (iv) functional sperm mitochondria as only live cells can retain the stain after washing. Scale bars = 20 μm Expression of steroidogenic pathway genes, hormone receptors, and secretory proteins in (**G**) ovaries from control and LHTN mice, n=6. Results are expressed as mean ± SEM, and statistical analysis consisted of a Student's t test. *P<0.05 vs control.